Thread the Needle: Genomics-guided Prompt-bridged Attention Model for Survival Prediction of Glioma based on MRI Images

Yi Zhong[1], Xubin Zheng[2](✉), Xiongri Shen[1], Jiaqi Wang[1], Leilei Zhao[1], Zhenxi Song[1], Zhiguo Zhang[1](✉)

[1] Harbin Institute of Technology, Shenzhen, China
{zoey24, xiongrishen, 23b951063, 24b951025}@stu.hit.edu.cn
{songzhenxi, zhiguozhang}@hit.edu.cn
[2] Guangdong Provincial Key Laboratory of Mathematical and Neural Dynamical Systems, School of Computing and Information Technology, Great Bay University, Dongguan, China
xbzheng@gbu.edu.cn

Abstract. Glioma remains one of the most lethal malignancy, making accurate prognosis crucial for personalized treatment and improved patient outcome. Existing models based on non-invasive magnetic resonance imaging (MRI) offer convenience, but they suffer from the poor performance and generalizability compared to genomic biomarkers, limiting their clinical adoption. Genomic biomarkers, such as IDH mutation and 1p/19q co-deletion, provide superior prognostic value but are restricted by their reliance on invasive surgical sampling. In this study, we hypothesize that these genomic biomarkers can guide the development of more robust MRI-based prognostic models, and propose a genomics-guided prompt learning framework that leverages both MRI and transcriptomic data to enhance survival prediction. Specifically, we introduce a novel visual modeling strategy for comprehensive glioma MRI representation and a Prompt-bridged Attention mechanism that can fuse multiple modalities during training and enhance visual representations during inference. Experimental results demonstrate that our proposed method achieves c-indeces of 0.6709 and 0.6904 on UCSF-PDGM and TCGA-GBM datasets, respectively, with highly significant p-values of 5.27×10^{-14} and 6.72×10^{-7}. These results substantially outperform existing methods, presenting a promising step toward reliable and non-invasive glioma prognosis prediction.

Keywords: Survival prediction · Prompt Learning · Genomics-Radiomics.

1 Introduction

Glioma is the most common and lethal primary malignancy in the central nervous system. [1] The highly heterogeneous prognosis of patients diagnosed with glioma, including extreme short- and long-term survival[2], renders optimal decision-making in clinical practice challenging. Improving survival prediction holds key

importance for achieving more informed clinical decision-making and personalized treatments. Although some molecular pathological biomarkers, such as isocitrate dehydrogenase (IDH) mutation and chromosome 1p/19q co-deletion status, can accurately prediction prognosis[3], these factors require invasive surgical sampling and expensive equipment. These shortcomings are the main barriers to the wide application of molecular pathological biomarkers in the prediction of glioma prognosis.

Magnetic resonance imaging (MRI) as a noninvasive alternative, plays a pivotal role in glioma diagnosis and treatment monitoring in clinical practice. Multiple studies[4, 5, 6] have underscored the prognostic value of deep learning derived MRI radiomic features in glioma patients. However, the use of radiomic features for survival prediction is susceptible to intra-institutional and inter-institutional imaging data heterogeneity, which results in poor generalization performance. In addition, the survival prediction using radiomic features is not as significant as using pathological molecules.

Some studies[7, 8, 9, 10, 11] have used MRI to identify molecular alterations of glioma patients, with accuracy of more than 85%. For example, Wu et al.[11] constructed a multi-task deep learning model to predict molecular alterations, grade, and prognosis of glioma patients. Other study[12] use the fusion of molecular status and radiomics for survival prediction. However, the multi-modal methods that fuse radiomics and molecular status, make no sense for prognostic prediction in a non-invasive way.

Therefore, we use genomic information to guide the MRI-based model only during the training process and redesign the representation of glioma MRI images to address the poor generalization performance and significance in predicting survival of glioma. We propose a genomics-guided prompt learning framework, in which prompt-bridged attention can realize multi-modal fusion between transcriptomic profiles and MRI images of glioma patients and enhance visual representations. Our main contributions are summarized as follows:

- We propose a genomics-guided prompt learning framework, to excavate gene-vision correlations affecting prognosis from unpair MRI and genetic data.
- We design a visual modeling strategy that can better representation of the glioma MRI images.
- The proposed Prompt-bridged Attention contains a prompt embedding token as bridge and gene-to-prompt and prompt-to-visual cross-attention to realize multi-modal fusion and enhance the unimodal representations of images.
- The experimental results and Kaplan-Meier analysis indicate that our proposed method achieves significant improvements in both robustness and significance of survival prediction, which is helpful for clinical treatment.

2 Methods

In this section, we present the overall description of our proposed genomics-guided prompt learning framework for excavating gene-vision correlations affecting prognosis from unpair MRI and genetic data. Then, we detail the data

processing and feature extraction for each modality. After that, we elaborate on the key components of our proposed framework.

2.1 Pairing MRI images and genetic data from different sources

We designed a method to pair these MRI images and bulk transcriptome data with survival state associations from different samples and different sources as much as possible. Based on the 2021 WHO classification of tumors of the central nervous system, we believe that if two samples have similar key clinical information, especially molecular pathology characteristics, they have similar survival risks. Thus, we organized each sample's clinical information into a textual description that included gender, age, survival time, and events, as well as molecular pathology information obtained through invasive methods. Then, we used BioClinicalBERT[13] to encode the caption to obtain a representation vector for each sample, and then performed cosine similarity calculations Sim<i,j> between the sample i from MRI images group and the sample j from the bulk transcriptome group. This method is only used to form our training data.

2.2 Visual modeling strategy for glioma MRI images

Previous studies [4, 5, 6] of using radiomics features for survival prediction have shown poor generalization and significance rather than using pathology or genomics due to the lack of heterogeneity between visual features of different survival subtypes and domain shift among datasets. Some studies[11, 14] used Class Activation Mapping (CAM) to visualize prognostic-related image regions in the output of model, found that the model focused mainly on the tumor core region with low-risk group while focused more on the edema region with high-risk group. Inspired by this finding, we design a visual modeling strategy that respectively encoding the tumor core regions and edema regions in the MRI image. Specifically, we use segmentation masks to extract the tumor core region and edema region from MRI images respectively, and then use ResNet-10 to encode them. Given the MRI image data $I_V \in \mathbb{R}^{4\times(H\times W\times D)}$ of a sample, the ResNet-10 as vision encoder is used to extract features from the tumor core region V_C and edema region V_E, the whole procedure of getting vision features f_v of input MRI image could be formulate as below:

$$\begin{aligned} f_c &= VisionEncoder(I_{core}) \in \mathbb{R}^{C_1\times(\frac{H}{4}\times\frac{W}{4}\times\frac{D}{4})} \\ f_e &= VisionEncoder(I_{edema}) \in \mathbb{R}^{C_1\times(\frac{H}{4}\times\frac{W}{4}\times\frac{D}{4})} \\ f'_c &= GlobalMaxpool(f_c) \\ f'_e &= GlobalMaxpool(f_e) \\ \mathbf{V} &= [f'_c, f'_v] \in \mathbb{R}^C, \end{aligned} \tag{1}$$

where H, W, D is the voxel size of input MRI image, C_1 is the dimension of encoded features and $C = 2 \times C_1$, $[\cdot]$ denotes the concatenate on last dimension. Notably, the low-level features (correspond to feature map is $1/4$ resolution of the input image) of ResNet-10 output is used as the representation.

2.3 Encoding gene expression based on transcriptomic data

We have collected transcriptome profiling of several glioma patient cohorts from some database[15, 16]. However, the cohort size of these datasets (less than 1k) is sparse compared to the feature dimension, i.e., the number of sequenced genes (usually 20k-60k), which leads to the potential problem of *curse of dimensionality*[17] when using the raw data to training. Therefore, it is imperative to preprocess the gene expression data to filter gene features. First, the multiple cohort datasets are combined together and the low expression genes with TPM mean values less than 1 are removed, which could be noise signals induced by sequencing techniques. Next, the gene expression data, represented as $log_2(TPM + 1)$, underwent filtering to exclude genes with standard deviation (SD) greater than 1, which are more affected by biological heterogeneity instead of gliomas. Then, the scFoundation[18] is used as encoder to convert the gene expression data to a gene embedding, which can also helps to remove the batch effect cross multiple datasets. Finally, a project module is introduced to align the dimensions of gene embedding with visual features. Given the gene expression data $I_G = \{g_1, g_2, \cdots, g_n\} \in \mathbb{R}^N$ of a sample, the encoded gene embedding is $G \in \mathbb{R}^{N \times C}$:

$$\begin{aligned} F_g &= GeneEncoder(I_G) \in \mathbb{R}^{N \times C_2} \\ \mathbf{G} &= LN\big(\sigma(F_g M_g)\big) \in \mathbb{R}^{N \times C} \ , \end{aligned} \tag{2}$$

where N is the number of filtered gene, C_2 is the dimension of the gene embedding, C corresponds to the dimension of the visual features $\mathbf{V}$, σ denotes the GELU[19] activation function, LN denotes performing layer normalization[20] on last dimension of the matrix, $M_g \in \mathbb{R}^{C_2 \times C}$ is the project matrix.

2.4 Prompt Bridge Attention with visual & Gene features

Once the visual features $\mathbf{V}$ and genetic features $\mathbf{G}$ have been encoded and dimension alignment, the next step is fusing the visual and genetic features together. In this section, we propose a Prompt-bridged Attention method for multi-modal fusion during training and enhanced visual representations during inference. Different from previous works using cross-attention mechanism that computing between the image features and gene embedding, the computing of cross-attention is divided into two parts in our proposed method. Specifically, a learnable prompt embedding $\mathbf{P} \in \mathbb{R}^{m \times d}$ (bridge prompt embedding in Fig 1) is introduced to learn critical features from gene embedding by Genetic-to-prompt (G2P) Attention and inject visual-genetic related knowledge into visual features by Prompt-to-visual (P2V) Attention. It is worth noting that the G2P Attention is only computed to inject features into the prompt during the training:

$$\begin{aligned} \mathcal{A}_{g2p} &= \text{Softmax}\left(\frac{(\mathbf{P}W_p) \times (\mathbf{G}W_g)^T}{\sqrt{d}}\right) \cdot (\mathbf{G}U_g) \\ \mathcal{A}'_{g2p} &= \mathbf{P} + \text{LN}(\mathcal{A}_{g2p}) \\ \mathcal{H}_g &= \text{Sigmoid}(\mathcal{A}'_{g2p}W_o) \ , \end{aligned} \tag{3}$$

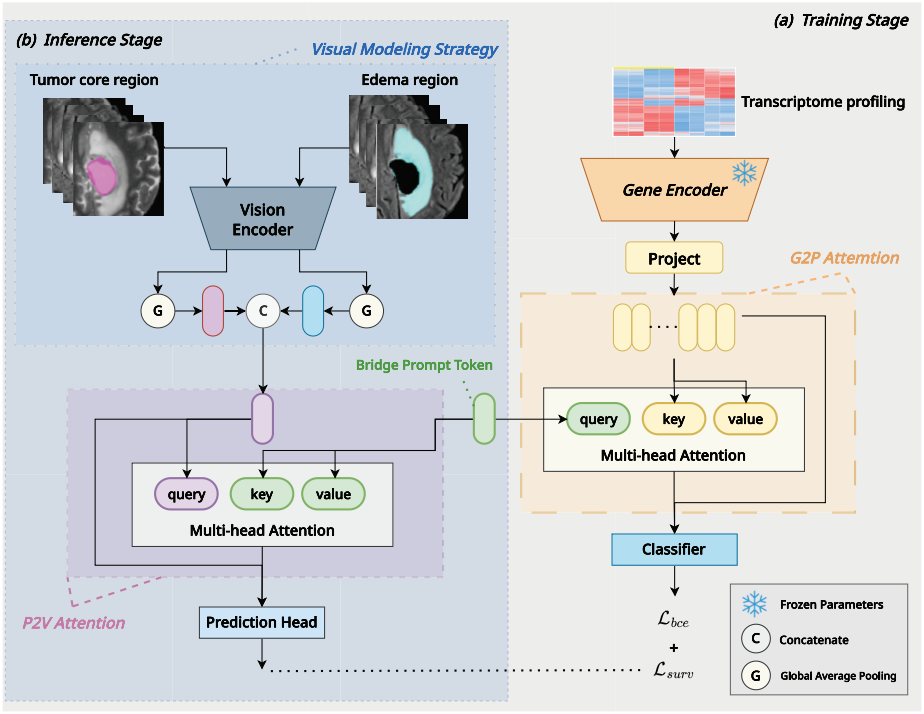

Fig. 1. The overview of the our proposed method. The model has different forward propagation processes during (a) training stage and (b) inference stage. The visual modeling strategy in the proposed methods is used to represent glioma MRI images, and the prompt-bridged attention is used to realize multi-modal fusion between transcriptomic profiles and MRI images of glioma patients in the training and enhance visual representations during inference. It is noted that the genetic branch is only used during training. Different optimizer targets are used for the visual branch (left region in this figure) and genetic branch (right region in this figure).

where $W_p, W_g, U_g \in \mathbb{R}^{d\times d}$ and $W_o \in \mathbb{R}^{d\times 1}$ are learnable parameters.

After that, the P2V Attention is computed to inject visual-genetic related knowledge into visual features from prompt embedding $\mathbf{P}$:

$$\begin{aligned} \mathcal{A}_{p2v} &= \text{Softmax}\left(\frac{(\mathbf{V}Z_v)\times(\mathbf{P}Z_p)^T}{\sqrt{d}}\right)\cdot(\mathbf{G}K_p) \\ \mathcal{A}'_{p2v} &= \mathbf{V} + \text{LN}(\mathcal{A}_{p2v}) \\ \mathcal{H}_v &= \mathcal{A}'_{p2v}Z_o \ , \end{aligned} \tag{4}$$

where $Z_p, Z_v, K_p \in \mathbb{R}^{d\times d}$ and $Z_o \in \mathbb{R}^{d\times 1}$ are learnable parameters.

To avoid modal interference caused by unpaired data, the output $\mathcal{H}_v$ and $\mathcal{H}_g$ have different optimizer targets. The output of gene branch $\mathcal{H}_g$ is supervised by

risk label R (binary label, risk or high, which is correspond to the risk group of samples from genomics cohort) and uses binary cross entropy as the loss function:

$$\mathcal{L}_{bce} = \frac{1}{N}\sum_{i=1}^{N} R\log(\mathcal{H}_g + (1-R)\log(1-\mathcal{H}_g), \tag{5}$$

while the output of vision branch $\mathcal{H}_p$ is supervised by overall survival times and death censorship, the negative log partial likelihood loss (NLL loss)[14] would be used as loss function:

$$\mathcal{L}_{surv} = -\frac{1}{N_{E=1}}\sum_{i:E_i=1}\left(\mathcal{H}_v - \log\sum_{j\in\Re(T_i)}\exp(\mathcal{H}_v)\right) , \tag{6}$$

where T_i, E_i are the event time and event indicator respectively. where $N_{E=1}$ is the number of patients with an observable event, the risk set $\Re(T_i)$ is the set of patients still at risk of failure at time t. The total loss $\mathcal{L}$ is the sum of binary cross entropy loss plus NLL loss: $\mathcal{L} = \mathcal{L}_{bce} + \mathcal{L}_{surv}$.

3 Experiments

3.1 Datasets

In this paper, we use three MRI datasets for training, including BraTS-TCGA-LGG(n=61)[21, 22], UPENN-GBM(n=609)[23, 24] and CPTAC-GBM(n=22)[25, 26], while the UCSF-PDGM(n=494)[27, 28] and BraTS-TCGA-GBM(n=96)[22, 28] are used as external test data for evaluating all methods. It is important to note that the datasets for training and test are collected from different centers and studies, which is very challenging for the generalization ability of the model. For genomic data, we have collected transcriptome profiling from four cohorts, including TCGA-LGG(n=513)[21],TCGA-GBM(n=160)[21], CPTAC-GBM(n=203)[26] and CGGA(n=970)[16]. It is important to note that the genetic data is used only in the training stage of our proposed method.

3.2 Metrics

We use c-index as evaluation metrics. The c-index, also known as the concordance index, is a metric used to evaluate the performance of survival analysis models. It measures the ability of a model to correctly order pairs of individuals in terms of their predicted survival times. The c-index can be formulated as follows:

$$\text{c-index} = \frac{1}{n(n-1)}\sum_{i=1}^{n}\sum_{j=1}^{n} I(T_i < T_j)(1-c_j) , \tag{7}$$

where n is the number of cases, T_i and T_j are the survival times of i-th patient and j-th patient. $I(\cdot)$ is the indicator function, which takes the value 1 if its argument is true, and 0 otherwise. c_j is the right censorship status.

Besides, we utilize Kaplan-Meier analysis[29] to visualize the survival events of all patients, analysis results are shown in Fig 2. We stratify all patients into low risk and high risk group according mid-value of the predicted risk scores from methods. Meanwhile, we also utilize Log-rank test[30] (p-value) to measure the statistical significance between the overall survival time of the low risk and high risk group. A p-value of 0.05 or lower is considered statistically significant.

3.3 Comparison Studies

As we can see from Table 1, our proposed method achieves best performance on both UCSF-PDGM and TCGA-GBM datasets. The method proposed by Wu et al. achieved the best results among the previous methods. Compared to method proposed by Wu et al., our proposed method improves the c-index by 9.48% on the UCSF-PDGM dataset and 8.83% on the TCGA-GBM dataset. In addition, our proposed method is highly significant in distinguishing high-risk group from low-risk groups, with p-values of 5.27×10^{-14} and 6.72×10^{-7} on UCSF-PDGM and TCGA-GBM, respectively, both much smaller than 0.05.

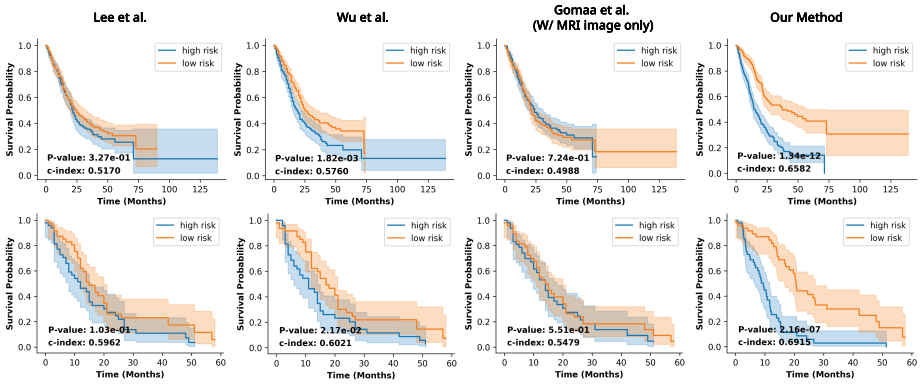

Fig. 2. The Kaplan-Meier analysis results of methods in comparison studies. Figures of the first row are the results on UCSF-PDGM dataset and the second row are the results on TCGA-GBM dataset. The shadow of the curve represents the confidence interval of the c-index.

3.4 Ablation Studies

In this section, we conducted several extra experiments to further discuss the impacts of visual modeling strategy and prompt-bridged attention in our proposed method. The results are shown in Table 2.

Table 1. Comparison studies on test datasets. Method and results using gray fonts are not included as one of the comparison experiments for the uni-modal methods

Methods	UCSF-PDGM		TCGA-GBM	
	c-index ↑	p-value ↓	c-index ↑	p-value ↓
Lee et al.[6]	0.5169	3.27×10^{-1}	0.5962	1.03×10^{-1}
Wu et al. [11]	0.5761	1.82×10^{-3}	0.6021	2.17×10^{-2}
Gomaa et al.† [12]	0.4988	7.24×10^{-1}	0.5479	5.51×10^{-1}
Gomaa et al.*[12]	0.6395	2.02×10^{-19}	0.4499	7.82×10^{-1}
Our Method	**0.6709**	$\mathbf{5.27 \times 10^{-14}}$	**0.6904**	$\mathbf{6.72 \times 10^{-7}}$

† Inference with MRI images only.
* Inference with MRI images and molecular information.

Table 2. Ablation Studies of our proposed method. The *VMS* denotes the **V**isual **M**odeling **S**trategy in the proposed method. The *BP*, A_{g2p} and A_{p2v} stand for **B**ridge **P**rompt, **G2P A**ttention and **P2V A**ttention respectively, which are the key components of Prompt-bridged Attention in our proposed method.

Train Data	Components					UCSF-PDGM		TCGA-GBM	
	VMS[1]	BP[2]	A_{g2p}[3]	A_{p2v}[4]	SG[5]	c-index ↑	p-value ↓	c-index ↑	p-value ↓
MRI	×	×	×	×	×	0.5516	3.07×10^{-2}	0.5747	2.13×10^{-1}
MRI	✓	×	×	×	×	0.6506	2.51×10^{-8}	0.6554	1.57×10^{-3}
MRI	✓	✓	×	✓	×	0.6453	1.97×10^{-10}	0.6479	1.03×10^{-3}
MRI+Gene	✓	✓	✓	✓	×	0.6339	2.57×10^{-9}	0.6672	7.57×10^{-5}
MRI+Gene	✓	✓	✓	✓	✓	**0.6709**	$\mathbf{5.27 \times 10^{-14}}$	**0.6904**	$\mathbf{6.72 \times 10^{-7}}$

[1] *VMS* stands for Visual Modeling Strategy.
[2] *BP* stands for Bridge Prompt.
[3] A_{g2p} represents G2P Attention in Fig 1.
[4] A_{p2v} represents P2V Attention in Fig 1.
[5] *SG* stands for Supervised Gene branch.

Impacts of Visual Modeling Strategy. Compared to the baseline model(the first row in Table 2), the visual modeling strategy for glioma MRI images contributed the greatest performance improvement in all components. Besides, our method based on the strategy only could well outperform the compared methods, which proves the strategy is so effective.

Impacts of Prompt-bridged Attention. We have two major observations from last two rows in Table 2. First, the components (*BP*, A_{g2p} and A_{p2v}) contained in Prompt-bridged Attention do not exist independently, but function in combination. Adding single of them does not improve performance. Second, supervised Gene branch(*SG*) makes Prompt-bridged Attention work properly and further improve the performance, which helps to eliminate the information damage during multi-modal fusion caused by sample-sample mismatch and maintain feature representation of Gene branch.

4 Conclusion

In this paper, we propose a genomics-guided prompt learning framework for survival prediction from glioma MRI images, in which the visual modeling strategy is used to conduct significantly feature representation of glioma MRI images and the prompt-bridged attention module is designed to learn visual-genetic correlations from unpaired MRI images and genetic data and enhancing visual representations during the inference procedure. The experimental results on the UCSF-PDGM and TCGA-GBM datasets indicate that our proposed method achieves significant improvements in both robustness and significance of survival prediction. Besides, the Kaplan-Meier analysis suggests that the predicted risk scores from the model could serve as a significant marker to distinguish high-risk and low-risk groups in glioma patients, which is helpful for clinical treatment.

Acknowledgments. This work was partly supported by the National Natural Science Foundation of China (No.: 32300554) and Guangdong Provincial Key Laboratory of Mathematical and Neural Dynamical Systems (No.: 2024B1212010004). The computational resources are supported by SongShan Lake HPC Center (SSL-HPC) in Great Bay University.

Disclosure of Interests. The authors have no competing interests to declare that are relevant to the content of this article.

References

[1] Shuli Liang et al. "Clinical practice guidelines for the diagnosis and treatment of adult diffuse glioma-related epilepsy". In: *Cancer medicine* 8.10 (2019), pp. 4527–4535.

[2] Quinn T Ostrom et al. "Adult glioma incidence and survival by race or ethnicity in the United States from 2000 to 2014". In: *JAMA oncology* 4.9 (2018), pp. 1254–1262.

[3] David N Louis et al. "The 2021 WHO classification of tumors of the central nervous system: a summary". In: *Neuro-oncology* 23.8 (2021), pp. 1231–1251.

[4] Nathaniel Braman et al. "Vascular network organization via Hough transform (VaNgOGH): a novel radiomic biomarker for diagnosis and treatment response". In: *International Conference on Medical Image Computing and Computer-Assisted Intervention*. Springer. 2018, pp. 803–811.

[5] Hyemin Um et al. "Impact of image preprocessing on the scanner dependence of multi-parametric MRI radiomic features and covariate shift in multi-institutional glioblastoma datasets". In: *Physics in Medicine & Biology* 64.16 (2019), p. 165011.

[6] Jung Oh Lee et al. "Added prognostic value of 3D deep learning-derived features from preoperative MRI for adult-type diffuse gliomas". In: *Neuro-oncology* 26.3 (2024), pp. 571–580.

[7] Burak Kocak et al. "Radiogenomics of lower-grade gliomas: machine learning–based MRI texture analysis for predicting 1p/19q codeletion status". In: *European radiology* 30 (2020), pp. 877–886.

[8] Yoon Seong Choi et al. "Fully automated hybrid approach to predict the IDH mutation status of gliomas via deep learning and radiomics". In: *Neuro-oncology* 23.2 (2021), pp. 304–313.

[9] Jing Yan et al. "Quantitative MRI-based radiomics for noninvasively predicting molecular subtypes and survival in glioma patients". In: *NPJ Precision Oncology* 5.1 (2021), p. 72.

[10] Guanzhang Li et al. "An MRI radiomics approach to predict survival and tumour-infiltrating macrophages in gliomas". In: *Brain* 145.3 (2022), pp. 1151–1161.

[11] Xuewei Wu et al. "Biologically interpretable multi-task deep learning pipeline predicts molecular alterations, grade, and prognosis in glioma patients". In: *NPJ Precision Oncology* 8.1 (2024), p. 181.

[12] Ahmed Gomaa et al. "Comprehensive multimodal deep learning survival prediction enabled by a transformer architecture: a multicenter study in glioblastoma". In: *Neuro-Oncology Advances* 6.1 (2024), vdae122.

[13] Emily Alsentzer et al. "Publicly Available Clinical BERT Embeddings". In: *NAACL HLT 2019* (2019), p. 72.

[14] Richard J Chen et al. "Multimodal co-attention transformer for survival prediction in gigapixel whole slide images". In: *Proceedings of the IEEE/CVF international conference on computer vision*. 2021, pp. 4015–4025.

[15] Allison P Heath et al. "The NCI genomic data commons". In: *Nature genetics* 53.3 (2021), pp. 257–262.

[16] Zheng Zhao et al. "Chinese Glioma Genome Atlas (CGGA): a comprehensive resource with functional genomic data from Chinese glioma patients". In: *Genomics, proteomics & bioinformatics* 19.1 (2021), pp. 1–12.

[17] Dylan Feldner-Busztin et al. "Dealing with dimensionality: the application of machine learning to multi-omics data". In: *Bioinformatics* 39.2 (2023), btad021.

[18] Minsheng Hao et al. "Large-scale foundation model on single-cell transcriptomics". In: *Nature Methods* (2024), pp. 1–11.

[19] Dan Hendrycks and Kevin Gimpel. "Gaussian error linear units (gelus)". In: *arXiv preprint arXiv:1606.08415* (2016).

[20] Jimmy Lei Ba, Jamie Ryan Kiros, and Geoffrey E Hinton. "Layer normalization". In: *arXiv preprint arXiv:1607.06450* (2016).

[21] Spyridon Bakas et al. "Advancing the cancer genome atlas glioma MRI collections with expert segmentation labels and radiomic features". In: *Scientific data* 4.1 (2017), pp. 1–13.

[22] Spyridon Bakas et al. *Segmentation labels and radiomic features for the pre-operative scans of the TCGA-LGG collection [Data Set]. The Cancer Imaging Archive*. 2017.

[23] Spyridon Bakas et al. "Multi-parametric magnetic resonance imaging (mpMRI) scans for de novo Glioblastoma (GBM) patients from the University of Pennsylvania Health System (UPENN-GBM)". In: *The Cancer Imaging Archive* (2021).

[24] Spyridon Bakas et al. "The University of Pennsylvania glioblastoma (UPenn-GBM) cohort: advanced MRI, clinical, genomics, & radiomics". In: *Scientific data* 9.1 (2022), p. 453.

[25] National Cancer Institute Clinical Proteomic Tumor Analysis Consortium et al. *The Clinical Proteomic Tumor Analysis Consortium Glioblastoma Multiforme Collection (CPTAC-GBM)(Version 16)[Data set]. The Cancer Imaging Archive. 2018*.

[26] Jingxian Liu et al. "Multi-scale signaling and tumor evolution in high-grade gliomas". In: *Cancer cell* 42.7 (2024), pp. 1217–1238.

[27] E Calabrese et al. "The University of California San Francisco Preoperative Diffuse Glioma MRI (UCSF-PDGM)(Version 4)". In: *The Cancer Imaging Archive* 10 (2022).

[28] Spyridon Bakas et al. "Segmentation Labels for the Pre-operative Scans of the TCGA-LGG collection". In: *The cancer imaging archive* (2017).

[29] Edward L Kaplan and Paul Meier. "Nonparametric estimation from incomplete observations". In: *Journal of the American statistical association* 53.282 (1958), pp. 457–481.

[30] J Martin Bland and Douglas G Altman. "The logrank test". In: *Bmj* 328.7447 (2004), p. 1073.